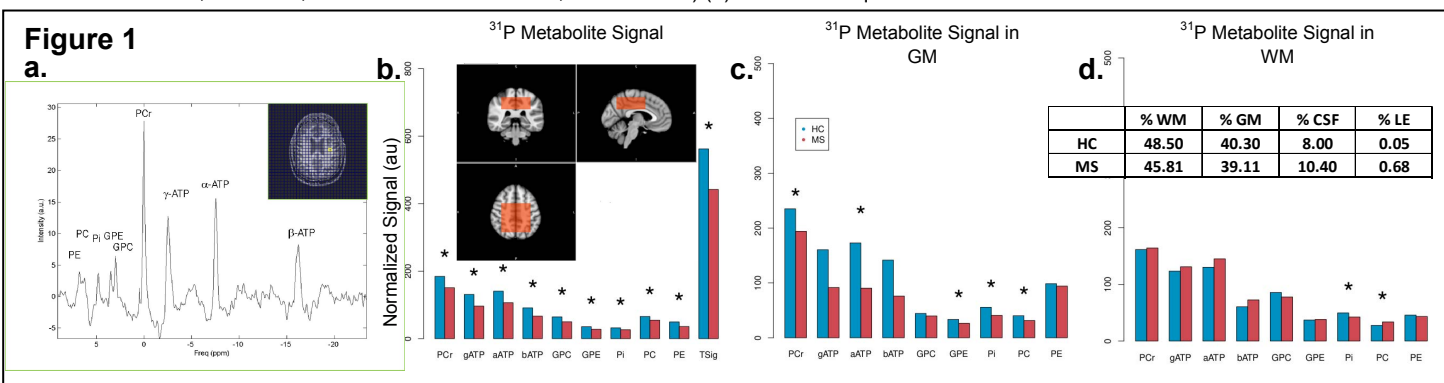


A 7T Combined ^{31}P Spectroscopy and ^1H MRI Study in Multiple Sclerosis

Manoj K Sammi¹, Yosef A Berlow^{1,2}, Thomas M Barbara¹, Audrey H Selzer¹, John W Grinstead³, Edward Kim⁴, Dennis Bourdette⁴, and William D Rooney^{1,2}
¹Advanced Imaging Research Center, Oregon Health & Science University, Portland, OR, United States, ²Department of Behavioral Neuroscience, Oregon Health & Science University, Portland, OR, United States, ³Siemens Medical Solutions, Portland, OR, United States, ⁴Department of Neurology, Oregon Health & Science University, Portland, OR, United States

Introduction: The association between mitochondrial dysfunction and neurodegeneration in multiple sclerosis (MS) is unclear. Neurodegeneration as evidenced by gray matter loss is an early feature of MS (1, 2). ^{31}P magnetic resonance spectroscopy and imaging (MRSI) provides a non-invasive measure of high energy phosphates and may serve as a surrogate marker for altered cerebral metabolism in brain disorders. The focus of this study was to investigate phosphorous metabolite differences between healthy control (HC) and MS subjects while correcting for partial volume effects by accounting for the signal contributions from gray matter (GM), white matter (WM), lesions (LE) and skeletal muscle (SM).

Methods: HC [n=11, 6 women and 5 men, 48 \pm 10 years] and MS subjects [n=9, 7 women and 2 men, 47 \pm 10 years, RRMS, EDSS scores: 2-6] were studied under an IRB-approved protocol. MR data acquisitions were performed on a 7T Siemens MAGNETOM system using a singly-tuned 8-channel phased-array ^1H (Rapid Biomedical), ^1H loop ("Halo") (3) and a sixteen-leg modified high-pass birdcage ^{31}P RF coils(4). Four sets of whole brain IR-prepared images were acquired at T_1 (ms) = 300, 900, 2000 and without inversion pulse for T_1 determination and tissue segmentation (FOV: 192x256x192 mm³, Data matrix: 192x256x96, TR=2.5 s, TE=2.3 ms). In addition, high resolution 3D data sets with MPRAGE (TR=2.3 s, T_1 =1.05 s, flip angle=6°, isotropic resolution of 0.8 mm, data matrix: 320x320x208, TA: 10:45 min) and FLAIR sequences (TR=8 s, isotropic spatial resolution of 0.8 mm, T_1 =2.15 s, data matrix: 280x320x208, TA=9:38 min) (5) were also acquired.



After completion of the high-resolution $^1\text{H}_2\text{O}$ images, the subject was placed in the ^{31}P coil – a Siemens 3T ^1H birdcage coil retuned for ^{31}P and integrated with a home-built proton loop– "Halo" coil (3). The subject's head was carefully re-positioned in this novel integrated " ^{31}P /Halo coil" setup and referenced with laser markers to be in the same location. Scout images for co-registration purposes were acquired with the ^1H coil tuned to proton frequency. Subsequent phosphorus RF pulse calibration and CSI data acquisition were done using the ^{31}P coil.

A ^{31}P MRSI gradient-echo FID acquisition was performed with an echo time of 2.3 ms (FOV: 250x250mmx200 mm³, acquisition data matrix: 20x20x16, final matrix: 32x32x16, TR =300 ms, flip angle=24°). An optimized sinc RF pulse of 600 μs duration centered at PCr resonance frequency with a bandwidth-time product of 6.54 was used to uniformly excite the phosphorous metabolites and avoid signal contribution from outside the region of interest. This large bandwidth also minimized spatial mis-registration during the slab selection in z-direction (e.g. 1.4 mm dispersion between PCr and β -ATP peak). Averaging was performed using 3D- cosine-weighted spatial phase encoding to minimize the acquisition time while maintaining a high signal to noise ratio with total acquisition time of 37.5 minutes. Two low resolution MRSI acquisitions (FOV: 240x240x200mm³, acquisition data matrix: 12x12x10, final data matrix=16x16x16, TR=220 ms, TE=2.3 ms, TA=4.6 min) were acquired with different flip angles (10° and 20°) to map the B_1 -field at 120.3 MHz. **Figure 1a** shows a typical spectrum obtained from one of the 11.5 mL (effective volume) voxels.

High resolution quantitative T_1 maps and 3D ^{31}P MRSI data were co-registered using scout images from the ^1H coil using FSL routines (6-8). Quantitative $^1\text{H}_2\text{O}$ T_1 maps were used to segment brain and surrounding tissue into GM, WM, CSF, LE and SM. MRSI data were fit in the time domain using AMARES routine in jMRUI software (9, 10) for the main ^{31}P metabolite peaks (PCr, ATP, PC, PE, Pi, GPC, GPE). The fitted signal intensities were corrected for B_1 -inhomogeneity, relative T_1 -weighting (11) and normalized using transmitter reference voltage amplitude. Voxels were selected from a standard space (MNI) volume of interest (~160 mL) in the parietal supra-ventricular region (**Figure 1b**). Voxels with significant contributions from CSF (>20%) or SM (>1%) were excluded. Spectral fitting results from these 1685 voxels were analyzed using a linear mixed-effects regression model for tissue type dependence using R software: ($S_{\text{Metabolite}} = \text{GM} + \text{WM} + \text{Group} + \text{GM} \times \text{Group} + \text{WM} \times \text{Group} + \epsilon_{\text{Subject}} + \epsilon_{\text{random}}$). Average values of different tissue percentage contributions are indicated in **Figure 1d** table.

Results and Discussion: **Figures 1b-d** show normalized ^{31}P metabolite signals (peaks are marked with asterisk for $P<0.01$; total signal, tsig=PCr+ATP+GPC+GPE+Pi+PC+PE) in HC and MS subjects (left blue and right red bars for HC and MS subjects, respectively). There was a significant reduction in average phosphate metabolite levels in MS (21%) compared to HC (**Figure 1b** bar plot). Tissue dependence analysis found significant ($P=0.01$) decrease in several phosphorus metabolites including phosphocreatine (17%), adenosine triphosphate (43%), inorganic phosphate (Pi) (27%) and phosphorylcholine (22%) in GM in MS whereas WM showed no significant changes except for Pi and PC (**Figures 1c and 1d**). There are no significant differences in quantitative $^1\text{H}_2\text{O}$ T_1 values between the groups. These significant changes in energy metabolites in GM (but not WM) may identify tissue at risk or in the process of degeneration as evidenced by the reduced cortical thickness or GM volume found in literature in larger MS populations and it may act as a surrogate marker of early neurodegeneration.

Grant Support: NMSS CA 1055A3, NIH R01-NS04801, NIH/NCRR 3UL1RR024140-04S1, Oregon Opportunity.

References: 1. Fisher, Lee, Nakamura, Rudick, *Ann Neuro* **64**:255-265 (2008). 2. Peterson, Bo, Mork, Chang, Trapp, *Ann Neuro* **50**:389-400 (2001). 3. Barbara, Sammi, Rooney, Grinstead, *PISM* **19**:1896 (2011). 4. Sammi, Berlow, Barbara, Grinstead, Bourdette, Rooney, *PISM* **18**:3375 (2010). 5. Grinstead, Speck, Paul, Silbert, Perkins, Rooney, *PISM* **19**:3034 (2010). 6. Smith, *Hum Brain Mapp* **17**:143-55 (2002). 7. Jenkinson, Smith, *Med Image Anal* **5**:143-56 (2001). 8. Zhang, Brady, Smith, *Med Imag IEEE Trans* **20**:45-57 (2001). 9. Naressi, Couturier, Devos, Janssen, Mangeat, de Beer, Graveron-Demilly, *MRMPBM* **12**:141-52 (2001). 10. Vanhamme, van den Boogaart, Van Huffel, *JMR* **129**:35-43 (1997). 11. Lei, Zhu, Zhang, Ugurbil, Chen, *MRM* **49**:199-205 (2003).